

RESEARCH PAPER

Novel Porous Iron Molybdate Catalysts for Synthesis of Dimethoxymethane from Methanol: Metal Organic Frameworks as Precursors

Ali Dehghani, Maryam Ranjbar*, Ali Eliassi

Department of Chemical Technologies, Iranian Research Organization for Science and Technology (IROST), Tehran, Iran

ARTICLE INFO

Article History:

Received 12 December 2018

Accepted 15 February 2018

Published 1 March 2018

Keywords:

Alternative Fuels

Dimethoxymethane

Iron Molybdate Catalyst

Metal Organic Framework

Methanol Oxidation

ABSTRACT

As a novel performance, methanol gas conversion to dimethoxymethane (DMM) in one-step based on Fe-Mo-O (iron molybdate mixed oxides) catalysts with high surface area fabricated by metal organic frameworks (MOFs) precursors was improved. For this approach, at first, Fe(III) precursors (iron (III) 1,3,5-benzenetricarboxylate (MIL-100 (Fe) and iron terephthalate (MOF-235)) and Mo(VI) precursor ((NH₄)₆Mo₇O₂₄·4H₂O) were synthesized. The catalysts were characterized by X-ray diffraction (XRD), Fourier transform infrared spectroscopy (FT-IR), scanning electron microscopy (SEM), energy-dispersive X-ray spectroscopy (EDX), transmission electron microscopy (TEM) analysis, temperature programmed desorption (NH₃-TPD), dynamic light scattering (DLS) technique, Brunauer–Emmett–Teller analysis (BET) and inductively coupled plasma optical emission spectroscopy (ICP-OES) techniques. Application of MOFs as precursors was provided fabricated catalysts with high specific surface area which subsequently afforded higher selectivity and productivity of dimethoxymethane. Novel catalytic performances can be due to synergistic effect between Mo(VI) and Fe(III) species which leads to catalysts with porous structure. As a result, with a Mo:Fe molar ratio of 3, the best catalyst was obtained which exhibited 43% conversion, 92% selectivity and 39% yield, respectively.

How to cite this article

Dehghani A, Ranjbar M, Eliassi A. Novel Porous Iron Molybdate Catalysts for Synthesis of Dimethoxymethane from Methanol: Metal Organic Frameworks as Precursors. *Nanochem Res*, 2018; 3(1): 50-61. DOI: 10.22036/nrcr.2018.01.006

INTRODUCTION

Energy supply, its conversion and storage in a way that essentially protects the environment are of the great challenges for human being in the 21st century. For many years, the vast mankind consumption of fossil fuels (crude oil, coal and natural gas) as primary energy basis owing to their high energy density values and easy accessibility. However, this global pattern of energy source is unbalanced. In addition to the limited fossil-fuel supplies, the global warming issue demands a radical change in finding the renewable energy sources [1].

Dimethoxymethane (DMM), also recognized as methylal, with chemical formula of C₃H₈O₂ is a commercial chemical compound which has various applications in chemical industries. This compound can be achieved from methanol which produced itself from biomass. The methanol mainstream is presently gained from natural gas-based and coal-based synthesis gas (syngas) [2-6]. DMM and POMM are deliberated as substitute fuels for low-temperature fuel cells which are much safer than methanol, due to, e.g. seldom toxicity of DMM and POMM lower volatility [7,8]. Furthermore, concentrated formaldehyde solutions can be

* Corresponding Author Email: marandjbar@gmail.com

gained through the selective oxidation of DMM into formaldehyde compared to the conventional method (methanol to formaldehyde conversion) [9]. As a significant usage, DMM has been applied as an oxygenated additive to diesel fuel, especially reducing particle emissions, which is a serious danger for the human health [10,11].

DMM is conventionally fabricated by acetalization of formaldehyde and methanol over acidic catalysts. Nevertheless, mentioned method includes sophisticated procedures, severe corrosion of equipment, and high reaction temperature [12,13]. In addition, one step selective oxidation of methanol to DMM owing to the economic and environmental advantages of the process has attracted much attention [13]. In this context, improvement of the selective catalysts for the one step methanol to DMM partial oxidation is an exciting issue, and has gained great concern in the recent years [6,14]. Selective methanol oxidation to DMM characteristically includes two steps: methanol oxidation to formaldehyde on redox sites and formaldehyde condensation with another methanol molecule to form DMM on acidic sites of catalyst [13,15]. To achieve high DMM yield, a suitable bifunctional catalyst with balanced redox ability and acidic sites is demanded. Excessive redox property and insufficient acidic sites can lead to the abundant amount of methyl formate (MF) and oxycarbide, while extreme acidic sites would output a great amount of dimethyl ether (DME) [12,16]. A variety of catalysts such as iron molybdate mixed oxides [6], molybdenum-based catalysts [17], ruthenium oxides [18], rhenium oxides [19,20], heteropolyacids (HPAs) [21], and vanadium-based catalysts [22,23] have been employed for one step methanol oxidation to DMM.

Newly, Mickael Capron et al. have established one-step gas phase selective methanol conversion to DMM using a mixed iron molybdate oxides as a catalyst with low surface area, about $10 \text{ m}^2\text{g}^{-1}$, synthesized by the coprecipitation method. This catalyst in a fixed-bed reactor under unusual reaction conditions showed the highest productivity ever observed in the direct conversion of methanol to DMM ($4.6 \text{ kg}_{\text{DMM}} \text{ h}^{-1} \text{ kg}_{\text{cat}}^{-1}$ at 553 K) [6].

Metal-organic frameworks (MOFs) are innovative class of highly porous hybrid materials assembled with inorganic cation or clusters coordinated [24,25]. MOFs with tridimensional framework have ultimate characteristics such as porous structures with high surface area, tunable pore size, crystalline

open structure and suitable thermal stability [26,27]. One of the main applications of MOFs is their catalytic activity. There are numerous investigations based on the usage of MOFs as catalysts or catalyst support systems [28, 29]. Also MOFs have been used as precursors for preparation of nano-sized materials such as porous carbon [30,31] and metal oxides [32,33]. Finding the nano-sized materials with desired morphologies will become possible by selecting suitable MOF precursors with distinct morphologies under suitable operational situations [34].

In addition to the aforementioned benefits of the one step oxidation of methanol to DMM, the goal of this work is to advance the performance of Fe-Mo catalyst by using metal organic frameworks as precursors to synthesize catalysts with high surface area with different morphologies. For this purpose, MIL-100(Fe) and MOF-235 was synthesized as precursors for Fe(III) while $(\text{NH}_4)_6\text{Mo}_7\text{O}_{24} \cdot 4\text{H}_2\text{O}$ was employed as a Mo(VI) precursor. The fabricated catalysts were characterized to use for one step production of DMM from methanol.

EXPERIMENTALS

Materials and apparatus

All chemicals used in this project were of analytical reagent grade and purchased from Merck Company without any purification. Fe(III) and Mo(VI) contents were determined by inductively coupled plasma optical emission spectroscopy (ICP-OES) (Shimadzu ICPS-7000, Japan). For all X-ray diffraction (XRD) patterns reported in this study, XRD was performed under atmospheric conditions with a Philips X-Pert. FTIR spectra were documented by a Bruker IFS-66 FT-IR Spectrophotometer (Karlsruhe, Germany). Brunauer-Emmett-Teller (BET) surface area measurements and pore volumes were performed by Belsorp mini II Bel (Japan). Scanning electron microscopy (SEM) was performed by gently distributing the sample powder on the stainless steel stubs, using an SEM (KYKY-3200, Zhongguancun Beijing, China) instrument. Transmission electron microscopy (TEM) analysis was performed by LEO 912AB electron microscope. The elemental analysis of samples was achieved by energy-dispersive X-ray spectroscopy (EDX) (30XL, Philips Company, Holland). Catalyst process evaluation was performed in a catalyst testing system with a fixed bed reactor which was used in earlier work [35]. Dynamic light scattering (DLS) technique

was widely employed for sizing NPs in liquid phase using a BI-200 SM Goniometer Version 2 (Brookhaven Instrument Corp., Holtsville, NY, USA). The light scattered by the NPs was distinguished at 173°, in dynamic laser scattering. For electrophoretic mobility quantification, which is a correlation between the NPs velocity and the electric applied field, size distribution and mean size were considered. Also, zeta potential was restrained by DLS method and was used to investigate the stability of nanoparticles against aggregation.

Catalysts Fabrication

Synthesis of MOF-235

MOF-235 was prepared under autogenous pressure according to the previous reported method [36]. 0.21 g terephthalic acid (1.23 mmol) was dissolved in 60 ml DMF by stirring for 10 min. Afterward, 0.20 g $\text{FeCl}_3 \cdot 6\text{H}_2\text{O}$ (0.74 mmol) was added to the mixture and stirred for 5 min. At that moment, 30 ml of reaction mixture with 30 ml ethanol were moved to a Teflon-lined autoclave, sealed and placed in a preheated electric oven (353 K) for 12 h. Finally, an orange powder (MOF-235) was attained which was recovered by centrifugation and washed with a DMF-ethanol mixture at least three times. Afterwards, it was dried overnight at 423 K to eliminate DMF.

Synthesis of MIL-100 (Fe)

MIL-100(Fe) was produced at low temperature synthetic method (<373 K) at atmospheric pressure under reflux condition. HF, HNO_3 , trimesic acid, metallic iron, and H_2O were employed as reagents, then, a solution of Fe:trimesic acid:HF: HNO_3 : H_2O with composition of 1.0:1.0:2.0:0.5:100 was transferred into a PTFE flask while refluxed at 368 K for 12 h under vigorous stirring. After crystallization, the achieved powder was adequately purified by hot deionized water followed by drying at vacuum [37].

Synthesis of Fe-Mo catalysts

Iron molybdate catalysts with Mo:Fe mol ratio of 3:1 was produced with the aid of coprecipitation method. An aqueous solution containing 1.0 mol $(\text{NH}_4)_6\text{Mo}_7\text{O}_{24} \cdot 4\text{H}_2\text{O}$ (AHM) and 2.3 mol $\text{FeCl}_3 \cdot 6\text{H}_2\text{O}$ was prepared according to the previous procedure [6]. Initially, the $(\text{NH}_4)_6\text{Mo}_7\text{O}_{24} \cdot 4\text{H}_2\text{O}$ solution (pH ~ 5) was acidified with HCl to pH ~ 1. Afterwards, $\text{FeCl}_3 \cdot 6\text{H}_2\text{O}$ solution was added drop wise for 30 min to the AHM solution at a temperature

kept in the range of 323-333 K under vigorous stirring. The yellowish precipitate was agitated for 60 min in its mother liquor. Afterwards, the precipitate was recovered by decantation for several times to remove of chloride ions. As a final point, the precipitate was filtered and dried at 383 K for 4 h. The dried precipitate was calcined at 723 K for 2 h to produce Fe-MoI catalyst. The other catalysts were synthesized with MOF-235 and MIL-100(Fe) precursors and named as Fe-MoII and Fe-MoIII, respectively. An aqueous solution containing 1.7 mol AHM and 1.0 mol MOF-235 were employed for synthesis of Fe-MoII catalyst. On the other hand, 1.3 mol AHM and 1.0 mol MIL-100 (Fe) were used for the synthesis of Fe-MoIII catalyst. The resultant precipitates were maintained under vigorous stirring for 2 h to achieve homogenous solutions, and then, the mixtures evaporated at 303 K to dry. The attained precipitates were calcined at 723 K for 3 h. All catalysts' colors were light green, and the yields of products were 72 %, 58% and 63% for Fe-MoI, Fe-MoII and Fe-MoIII catalysts, correspondingly.

RESULT AND DISCUSSION

Characterization of the catalysts

FT-IR spectra

FT-IR spectra of MIL-100(Fe), MOF-235, FeMoI, FeMoII and FeMoIII were recorded by KBr pellet method. The peaks were attributed to C=O stretching vibration at 1713 and 1684 cm^{-1} in MIL-100(Fe) and MOF-235 indicating the presence of carboxylate linkers in their frameworks. The absorption bands due to C=C (1447, 1575 cm^{-1}) and C-H aromatic (3065 cm^{-1}) established the MIL-100(Fe) compound synthesis [37]. Furthermore, the FT-IR spectrum of MOF-235 comprises of the main vibrational bands at 554 cm^{-1} (Fe-O), 1110 and 776 cm^{-1} (C-H vibration of aromatic ring), 1286 cm^{-1} (C-O-C), and 1421 and 1568 cm^{-1} (C=C aromatic) which are in agreement with earlier reported values for MOF-235 [36]. The main characteristic bands at 853-894 cm^{-1} (Fe-O) and 612-635 cm^{-1} (Mo-O) in the FT-IR spectrum of catalysts were illustrated. This showed that the synthesis of all catalysts was performed properly.

SEM, EDX, TEM and DLS

The surface characterization results of Fe-MoI, Fe-MoII and Fe-MoIII morphology were achieved by SEM and TEM techniques accomplished by EDX analysis (Fig. 1 and Fig. 2a,b). EDX is an

important non-destructive analytical tool typically useful for the chemical composition; it is one of the electron microscopy procedures used for semi-quantitative analysis (bulk chemical elemental

analysis) using the backscattered electron mode. The bulk sediments were analyzed by EDX at low magnification by averaging the results of several spots. SEM-EDX analysis is frequently employed

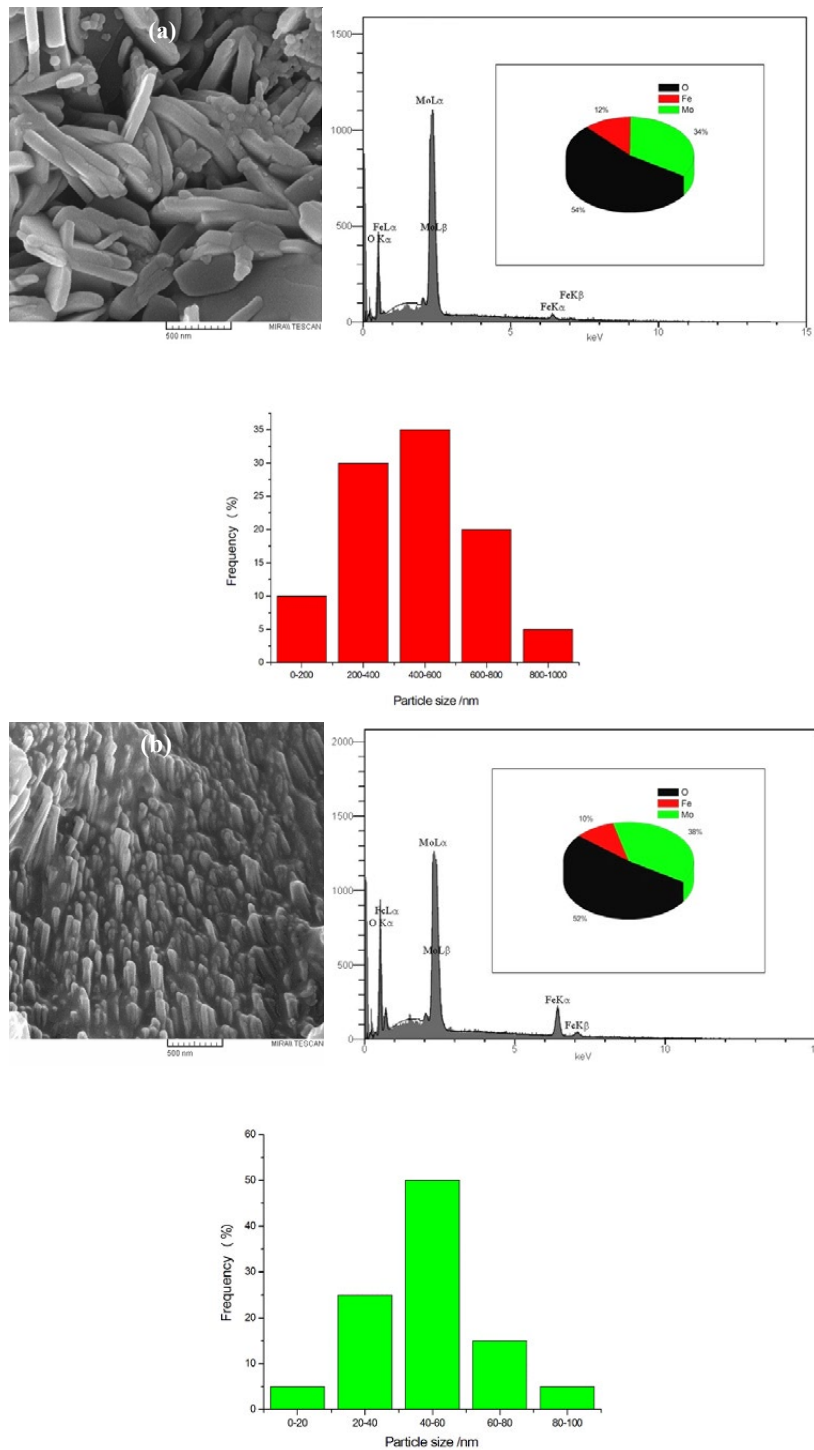


Fig. 1: SEM images of (a) Fe-MoI, (b) Fe-MoII and (c) Fe-MoIII and EDX accomplished by the size distribution histogram of the prepared catalysts.

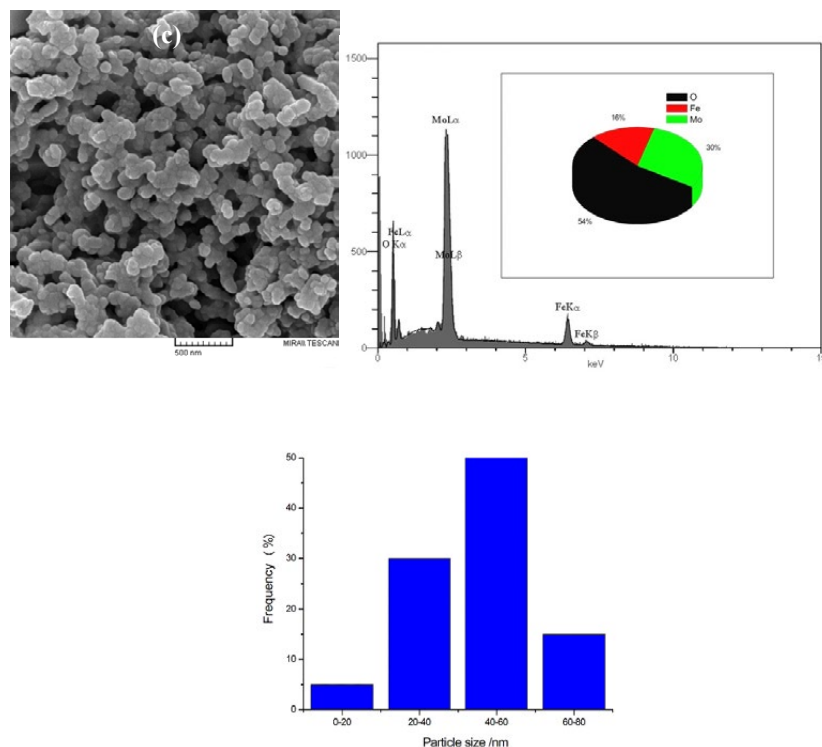


Fig. 1: SEM images of (a) Fe-MoI, (b) Fe-MoII and (c) Fe-MoIII and EDX accomplished by the size distribution histogram of the prepared catalysts.

to afford qualitative chemical analyses of elements present in the samples. As shown in Fig. 1 and Figs. 2a, and b, when metal organic frameworks are employed as precursors, the particle size of catalysts are reduced compared to Fe-MoI particles synthesized from $(\text{NH}_4)_6\text{Mo}_7\text{O}_{24}\cdot 4\text{H}_2\text{O}$ (AHM) and $\text{FeCl}_3\cdot 6\text{H}_2\text{O}$ directly. The SEM micrograph of Fe-MoI showed a non-uniform and disordered structure, while Fe-MoII and Fe-MoIII have nanorod and nanoparticle morphologies, respectively. The Fe-MoII and Fe-MoIII have more porosity compared with Fe-MoI structure (proved by BET and TEM microscopy), so more catalytic activity is expected. Size distribution histogram of the catalysts displays a relatively uniform distribution for Fe-MoII and Fe-MoIII nano catalysts while Fe-MoI catalyst shows non-uniform distribution of particles. Particle size can be measured by determining the random variations in the light intensity scattered from solution. This technique is generally identified as dynamic light scattering (DLS) but is also named photon correlation spectroscopy (PCS) and quasi-elastic light scattering (QELS). The size of nanoparticles was explored by DLS as can be seen in Fig. 2c (for Fe-MoII catalyst as the best catalyst). In general, the nanoparticle size spans

the range between 70 and 86 nm. In addition, zeta potential was restrained by DLS technique and was used to consider the stability of nanoparticles against aggregation. NPs with a zeta potential $\sim \pm 30$ mV have been exposed to be steady in suspension, as the surface charge inhibits aggregation of the particles (Fig. 2d).

X-ray diffraction patterns

The crystalline structure of MOFs and prepared catalysts were investigated by XRD technique (Fig. 3). The MOF-235 XRD pattern (Fig. 3b) exhibited high crystallinity with reflection patterns in the range of $5\text{-}40^\circ$ (2θ). The main characteristic peaks at $2\theta = 9.8, 10.6, 12.8, 17, 19$ and 23 were similar to MOF-235 standard data confirming the synthesis of MOF-235 [36]. As depicted in Fig. 3a, the MIL-100(Fe) diffraction patterns are observed in a small angle domain similar to published XRD patterns indicating the formation of MOF [37]. For Fe-Mo catalysts, three phases are expected; $\text{Fe}_2(\text{MoO}_4)_3$, MoO_3 , and $\beta\text{-FeMoO}_4$ components. The presence of three phases was approved by XRD analysis which is in accordance with the published literature [6] (Fig. 3c).

ICP-MS analysis

ICP-OES was regularly performed for the elemental analysis in a wide range of sample matrices for many years due to its relative ease of use, flexibility, low detection limits and low cost.

Furthermore, it needs shorter analysis time when equipped with a simultaneous-CCD detector (charge coupled device) as the one available in our laboratory. The ICP-MS measurements of fabricated catalysts were done in order to determine Mo:Fe

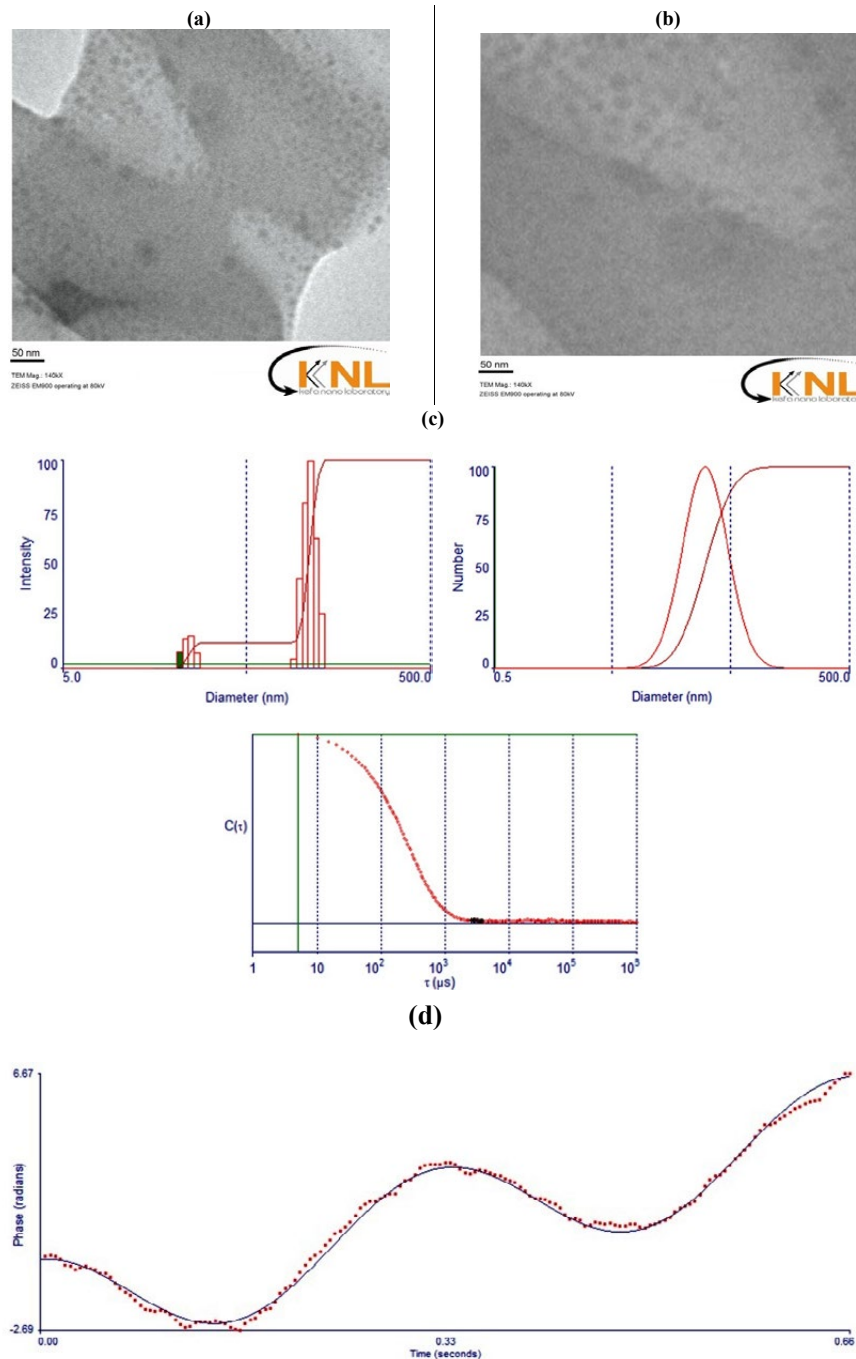


Fig. 2: TEM images of (a) Fe-MoII, (b) Fe-MoIII, (c) DLS results of size distributions, log normal size distributions, $C(\tau)$ of Fe-MoII, and (d) zeta potential of Fe-MoII catalyst.

ratios. The obtained Mo:Fe ratios were 2.9, 2.8, 2.8 for Fe-MoI, Fe-MoII, and Fe-MoIII, respectively, which are in a good agreement with the theoretical ratio of 3:1 (see Table 1).

BET analysis

BET surface area, Mo:Fe ratio, measured from ICP-MS and total pore volume of all catalysts are displayed in Table 1. The surface area of MOF-235 and MIL-100(Fe) were 981 and 1678 m²g⁻¹, respectively, according to previous reports [36,37].

These values decreased to 175 m²g⁻¹ (total pore volume = 0.38 cm³g⁻¹) and 213 m²g⁻¹ (total pore volume = 0.46 cm³g⁻¹) for Fe-MoII and Fe-MoIII that are derived from MOF-235 and MIL-100(Fe), correspondingly. The BET surface area of Fe-MoI was 8.9 m²g⁻¹ (total pore volume = 0.09 cm³g⁻¹) meaningfully lower than Fe-MoII and Fe-MoIII. Fig. 4 demonstrates the nitrogen adsorption-desorption isotherms of Fe-MoI, Fe-MoII and Fe-MoIII catalysts. According to IUPAC classification [38], the isotherm of Fe-MoI corresponds to

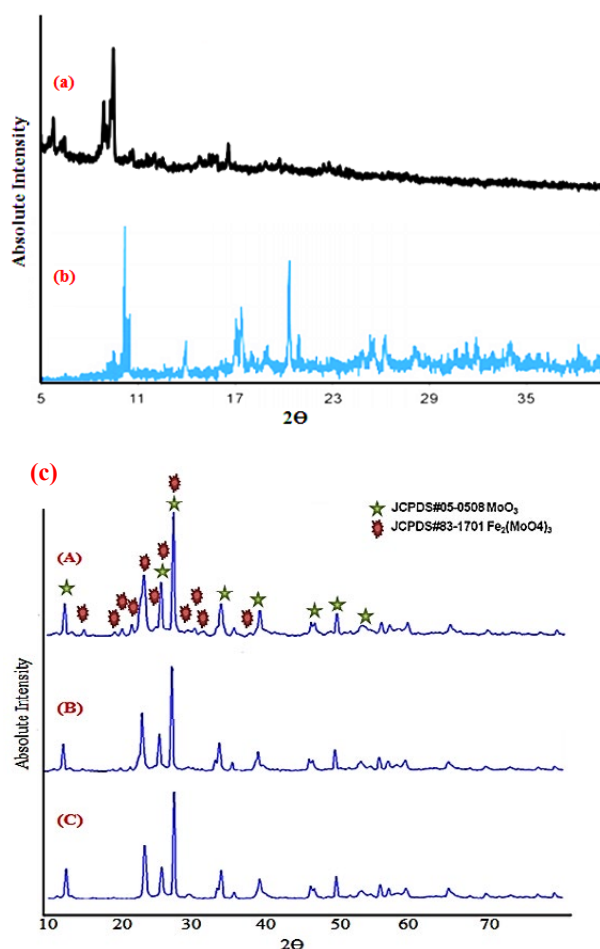


Fig. 3: XRD patterns of (a) MIL-100(Fe), (b) MOF-235 and (c) Fe-MoI (A), Fe-MoII (B) and Fe-MoIII (C).

Table 1. BET surface area, Mo/Fe ratio measured from ICP-MS and total pore volume of all catalysts.

Catalyst	Mo/Fe ratio		S _{BET} (m ² g ⁻¹)	Total pore volume (cm ³ g ⁻¹)
	Theoretical	ICP-MS		
Fe-MoI	3	2.9	8.9	0.09
Fe-MoII	3	2.8	175	0.38
Fe-MoIII	3	2.8	213	0.46

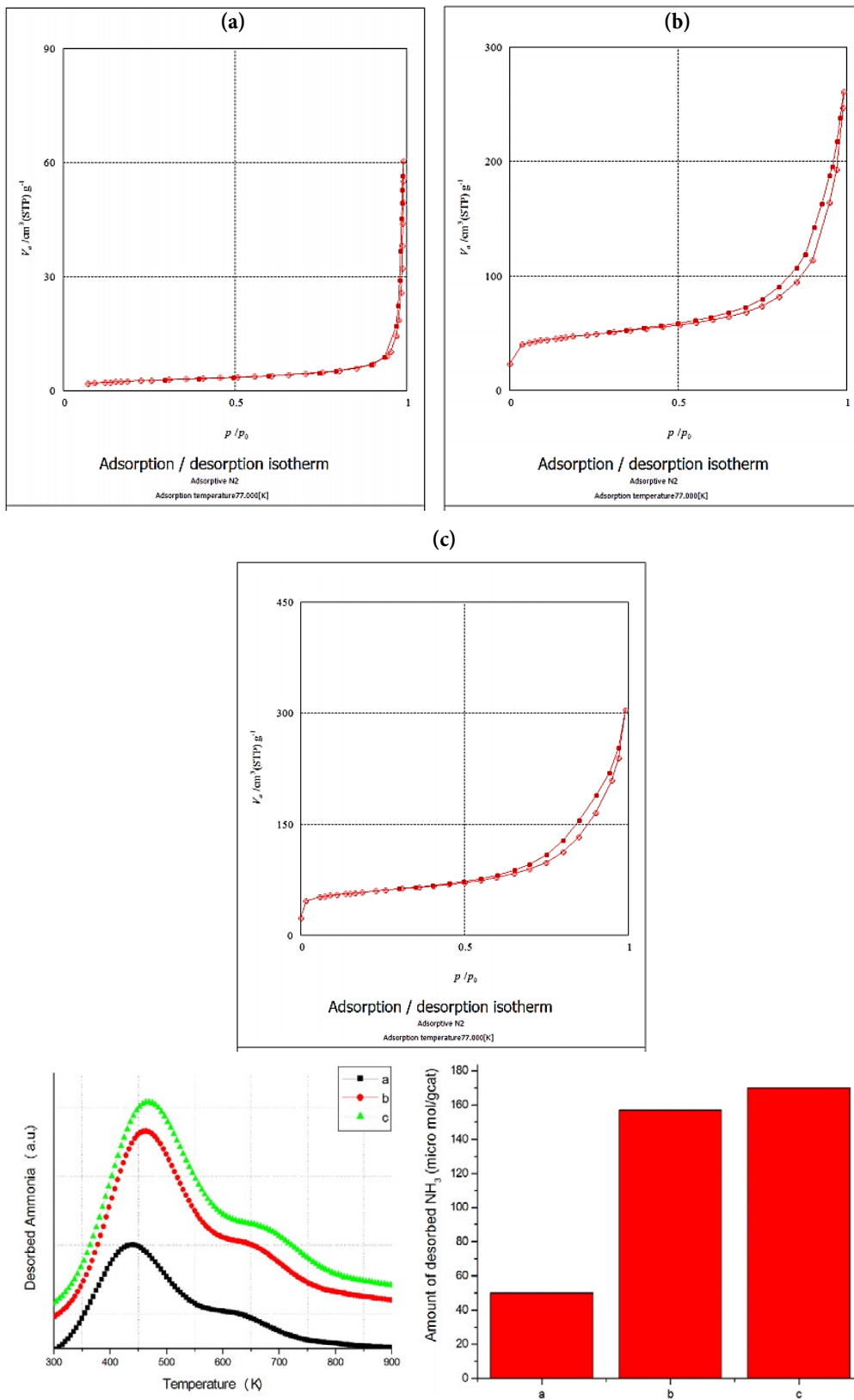


Fig. 4: Nitrogen adsorption-desorption isotherms for the (a) Fe-MoI, (b) Fe-MoII and (c) Fe-MoIII, and (d) NH_3 -TPD profiles of (a) Fe-MoI, (b) Fe-MoII, (c) Fe-MoIII accomplished by mount diagram.

nonporous and non-wetting solids (type III) with weak interaction between adsorbent and adsorbate. For Fe-MoII and Fe-MoIII, these isotherms correspond to type IV with an H3 hysteresis loop, characteristic of mesoporous structures with slit-shaped and non-rigid pores. The achieved data were established more porosity in the structure of Fe-MoII and Fe-MoIII compared with Fe-MoI. On the other hand, the catalytic activity of Fe-MoII was higher than that of Fe-MoIII which can be due to its nanorod structure. In fact, morphology of particles and shape of pores with different accessible active sites can be operative in activity of catalysts rather than the specific surface area only.

NH_3 -TPD spectra

NH_3 -TPD technique affords information on the strength and amount of acid sites by using NH_3 as a basic probe molecule. The peaks in the NH_3 -TPD profiles are classified to three types of acid sites with different acid strengths. The desorption peaks in Fig. 4d at ca. ~ 450 K is related to the weak acid sites.

Catalytic performance tests

Methanol conversion, DMM selectivity and DMM yield

In order to investigate the synthesized catalysts, at each experiment, 1.0 g of the catalyst was loaded into the reactor with stainless steel grid at both ends. For simulation of methanol:air condition, a ratio of $\text{CH}_3\text{OH}:\text{O}_2:\text{N}_2$ with 40/13/47 mol % was chosen. The gas hourly space velocity (GHSV) was adjusted to $16 \text{ NLh}^{-1}\text{g}_{\text{cat}}^{-1}$ (liquid methanol and air flow rates were controlled at 11 ml h^{-1} and 160 ml min^{-1} , respectively). The experiments were done at 503, 523, 543 and 563 K and the liquid products were guided to GC analyzer (Teif-Gostar co, Iran). All experiments were completed at atmospheric pressure. The reaction products were analyzed every 30 min until stabilization. On the basis of the results, the catalyst was stabilized after about 5 h. The main byproduct of reaction was formaldehyde (F), therefore the other byproducts were discarded. Methanol conversion, DMM selectivity and DMM yield were calculated according to the utilized formulas.

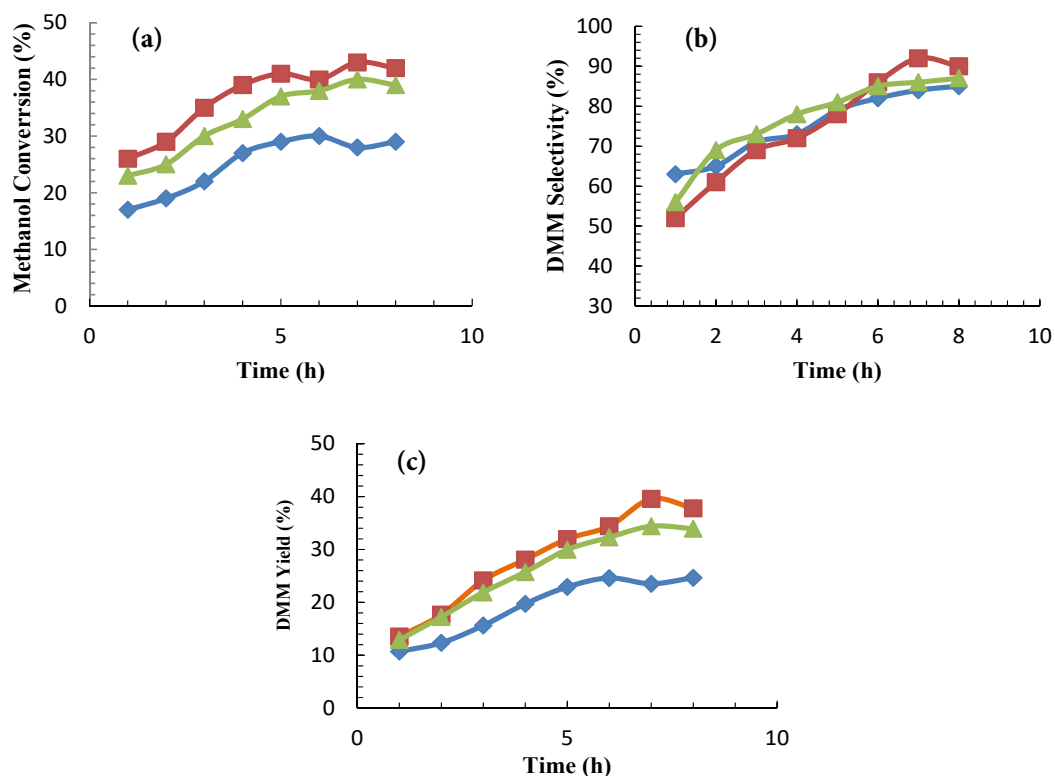


Fig. 5: Effect of reaction time on (a) methanol conversion, (b) DMM selectivity and (c) DMM yield over Fe-MoI (◆), Fe-MoII (■) and Fe-MoIII (▲) catalysts. Experimental conditions: GHSV = $16 \text{ NLh}^{-1}\text{g}^{-1}$, $T = 543 \text{ K}$, $\text{CH}_3\text{OH}/\text{O}_2/\text{N}_2 = 40/13/47 \text{ mol}\%$.

Methanol conversion (%) =

$$\frac{\text{mol (MeOH}_{\text{in}} - \text{MeOH}_{\text{out}})}{\text{mol (MeOH}_{\text{in}})} \times 100 \quad (1)$$

$$\text{DMM selectivity (\%)} = \frac{\text{mol (DMM}_{\text{out}})}{\text{mol (DMM}_{\text{out}} + \text{F}_{\text{out}})} \times 100 \quad (2)$$

$$\text{Yield (\%)} = (\text{Methanol conversion} \times \text{DMM selectivity}) \times 100 \quad (3)$$

Fig. 5a represents the catalytic performances of the catalysts at 543 K, which was the optimal temperature for DMM production based on Mickael Capron et al.'s report [6]. The methanol conversion gradually enhanced when reaction time increased. Fe-MoII and Fe-MoIII revealed the similar methanol conversion (ca 42 %), whereas Fe-MoI gave a 30 % conversion. The activity of Fe-MoII and Fe-MoIII catalysts were significantly higher than Fe-MoI, owing to their extra specific surface area with higher porosity compared to Fe-MoI.

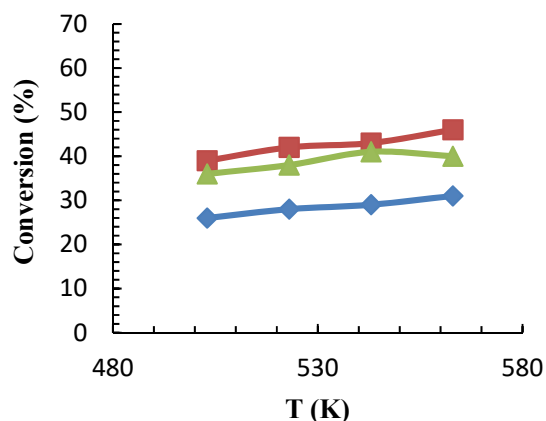


Fig. 6: Influence of reaction temperature on methanol conversion over Fe-MoI (◆), Fe-MoII (■) and Fe-MoIII (▲) catalysts. Experimental conditions: GHSV = 16 NLh⁻¹g⁻¹, CH₃OH/O₂/N₂ = 40/13/47 mol%.

The same trend was detected in the case of DMM selectivity evolution, which gradually increased with the reaction time up to 6 h (Fig. 5b). The highest DMM selectivity was perceived over Fe-MoII (92 %). Similarly, a high selectivity (87%) to DMM was achieved with Fe-MoIII. A significantly high DMM selectivity (85 %) was observed for Fe-MoI. The higher selectivity of Fe-MoII and Fe-MoIII can be explained by their higher surface area and active sites in comparison to Fe-MoI. DMM yield as a catalytic performance indicator also was investigated. As shown in Fig. 5c, when the reaction time increased from 1 to 7 h, the DMM yield was improved. Fe-MoII and Fe-MoIII offered higher DMM yield (39.56 and 34.4%) compared with Fe-MoI (24.65 %). Under this condition, DMM yield of Fe-MoII and Fe-MoIII was 39.56 and 34.4, respectively, which are much higher than that of Fe-MoI (24.65 %). All the prepared catalysts have the same Mo:Fe ratio (2.8-2.9), so higher performance of Fe-MoII and Fe-MoIII can be related to the more accessible

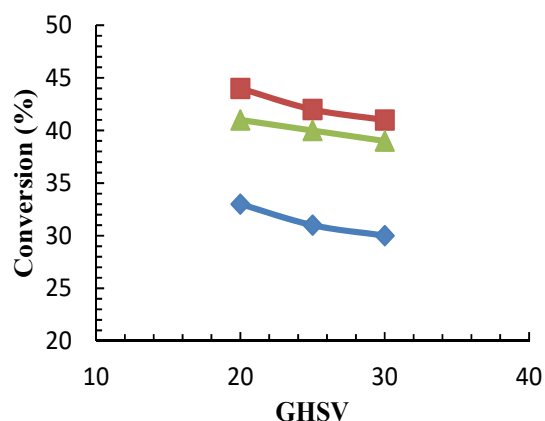


Fig. 7: Influence of GHSV on methanol conversion over Fe-MoI (◆), Fe-MoII (■) and Fe-MoIII (▲) catalysts. Experimental conditions: T = 543 K, CH₃OH/O₂/N₂ = 40/13/47 mol%.

Table 2. Comparison of catalyst activities between previous studies and the current study.

Catalyst	T _{optimal} (K)	MeOH Conv (%)	DMM Selectivity (%)	Yield (%)	Ref
Al-P-V-O	383	55.6	81.5	45.31	[13]
V ₂ O ₅ -MoO ₃ /Al ₂ O ₃	393	54.2	92.1	49.91	[12]
V ₂ O ₅ -TiO ₂ /Al ₂ O ₃	393	43	90.7	39	[16]
Sulfated Vanadia Titania	403	74	83	61	[2]
V-Ti-O	403	66	93	61.38	[2]
V ₂ O ₅ -CeO ₂	433	17	90	15.3	[2]
Re-TiO ₂	513	59.5	47	27.96	[2]
Re-ZrO ₂	513	35.8	32	11.45	[2]
Fe-Mo-O	528	46	85	39.1	[6]
Fe-Mo (MOF precursor)	543	43	92	39.56	This Work

active sites of these catalysts compared to Fe-MoI. A comparison between previous studies and the current study on methanol conversion, DMM selectivity and DMM yield is presented in Table 2.

Effect of the reaction temperature

Fig. 6 describes the reaction temperature effect on the methanol conversion over Fe-MoI, Fe-MoII, and Fe-MoIII catalysts. The main methanol oxidation products are DMM, formaldehyde, formic acid, methyl formate, and carbon oxides (CO and CO₂) [39,40]. However, for the Fe-Mo catalyst, main products were DMM and formaldehyde. The temperature affects the products distribution significantly. The methanol conversion enhanced by increasing temperature from 503 to 563 K. All catalysts are similar in the variance tendency of the methanol conversion with the temperature. Nevertheless, Fe-MoII and Fe-MoIII give a better methanol conversion than Fe-MoI. Porous structures with higher surface areas of Fe-MoII and Fe-MoIII catalysts lead to surface acidity with enhanced quantity and suitable strengths, which can promote the condensation reaction and hence give a positive effect on the methanol oxidation to produce DMM.

Effect of gas hourly space velocity (GHSV)

GHSV effect was explored in the range of 20-30 NLh⁻¹g_{cat}⁻¹. As shown in Fig. 7, methanol conversion decreased gradually with GHSV increasing from 20 to 30 NLh⁻¹g_{cat}⁻¹. The same behavior was distinguished for the studied catalysts while the highest methanol conversion was achieved for Fe-MoII. Using metal-organic frameworks, as appropriate precursors, is an excellent approach to arrange catalysts with high surface areas and more accessible active sites.

CONCLUSION

In this study, as a novel strategy, two metal-organic frameworks namely MOF-235 and MIL-100(Fe) were employed as precursors to fabricate porous iron molybdate mixed oxide catalysts for the gas phase selective conversion of methanol to DMM using a mixture of methanol and air as reactants. Three different catalysts were synthesized by the coprecipitation of MOF-235, MIL-100(Fe) and FeCl₃ with (NH₄)₆Mo₇O₂₄·4H₂O before being calcinated at 723 K in atmospheric pressure. MOF frameworks, as proper precursors, lead to formation of catalysts with higher specific surface areas,

subsequently higher selectivity, and productivity. Excellent catalytic performance can be ascribed to the synergetic redox and acid properties presented in the Fe-Mo-O catalyst, and porous structures of the catalysts with high accessible acid sites (related to the consecutive partial oxidation and condensation reactions).

ACKNOWLEDGEMENTS

Author acknowledges the support rendered by the Iranian Research Organization for Science and Technology (IROST) and Iran Nanotechnology Initiative Council (INIC) for this study.

CONFLICT OF INTEREST

The authors declare that there is no conflict of interests regarding the publication of this paper.

REFERENCES

- Poizat P, Dolhem F. Clean energy new deal for a sustainable world: from non-CO₂ generating energy sources to greener electrochemical storage devices. *Energy & Environmental Science*. 2011;4(6):2003-19.
- Thavornprasert K-a, Capron M, Jalowiecki-Duhamel L, Dumeignil F. One-pot 1,1-dimethoxymethane synthesis from methanol: a promising pathway over bifunctional catalysts. *Catalysis Science & Technology*. 2016;6(4):958-70.
- Dumeignil F, Capron M, Katryniok B, Wojcieszak R, Löfberg A, Girardon J-S, et al. Biomass-derived Platform Molecules Upgrading through Catalytic Processes: Yielding Chemicals and Fuels. *Journal of the Japan Petroleum Institute*. 2015;58(5):257-73.
- Doucet C, Germanaud L, Couturier JL, Dubois JL, Sage JM. Mélange de polyoxyméthylène dialkyléthers symétriques et leur utilisation dans des distallats hydrocarbonés. Google Patents; 2008.
- BARDON S, Gleize V, Romeyer J. Structure de filtration pour les gaz d'échappement d'un moteur a combustion interne. Google Patents; 2004.
- Thavornprasert K-a, Capron M, Jalowiecki-Duhamel L, Gardoll O, Trentesaux M, Mamede A-S, et al. Highly productive iron molybdate mixed oxides and their relevant catalytic properties for direct synthesis of 1,1-dimethoxymethane from methanol. *Applied Catalysis B: Environmental*. 2014;145:126-35.
- Chetty R, Scott K. Dimethoxymethane and trimethoxymethane as alternative fuels for fuel cells. *Journal of Power Sources*. 2007;173(1):166-71.
- Vigier F, Coutanceau C, Léger JM, Dubois JL. Polyoxymethylenedimethylether (CH₃O(CH₂O)_nCH₃) oxidation on Pt and Pt/Ru supported catalysts. *Journal of Power Sources*. 2008;175(1):82-90.
- Łojewska J, Wasilewski J, Terelak K, Łojewski T, Kołodziej A. Selective oxidation of methylal as a new catalytic route to concentrated formaldehyde: Reaction kinetic profile in gradientless flow reactor. *Catalysis Communications*. 2008;9(9):1833-7.
- Ball JC, Lapin C, Buckingham J, Frame E, Yost D, Garbak

- J, et al. Dimethoxy Methane in Diesel Fuel: Part 3. The Effect of Pilot Injection, Fuels and Engine Operating Modes on Emissions of Toxic Air Pollutants and Gas/Solid Phase PAH. SAE Technical Paper Series; 2001/09/24: SAE International; 2001.
11. The Effect of Dimethoxy Methane Additive on Diesel Vehicle Particulate Emissions. SAE Technical Paper Series; 1998/10/19: SAE International; 1998.
 12. Meng Y, Wang T, Chen S, Zhao Y, Ma X, Gong J. Selective oxidation of methanol to dimethoxymethane on V₂O₅-MoO₃/γ-Al₂O₃ catalysts. Applied Catalysis B: Environmental. 2014;160-161:161-72.
 13. Chen S, Meng Y, Zhao Y, Ma X, Gong J. Selective Oxidation of Methanol to Dimethoxymethane over Mesoporous Al-P-V-O Catalysts. AIChE Journal. 2013;59(7):2587-93.
 14. Kotbagi T, Nguyen DL, Lancelot C, Lamonier C, Thavornprasert KA, Wenli Z, et al. Transesterification of Diethyl Oxalate with Phenol over Sol-Gel MoO₃/TiO₂ Catalysts. ChemSusChem. 2012;5(8):1467-73.
 15. Selective oxidation of methanol to dimethoxymethane under mild conditions over V₂O₅/TiO₂ with enhanced surface acidity. Chemical Communications. 2007(21):2172.
 16. Meet Our Authors. MRS Bulletin. 2015;40(12):1009-18.
 17. Rocchiccioli-Deltcheff C, Aouissi A, Launay S, Fournier M. Silica-supported 12-molybdophosphoric acid catalysts: Influence of the thermal treatments and of the Mo contents on their behavior, from IR, Raman, X-ray diffraction studies, and catalytic reactivity in the methanol oxidation. Journal of Molecular Catalysis A: Chemical. 1996;114(1-3):331-42.
 18. Selective Oxidation of Methanol and Ethanol on Supported Ruthenium Oxide Clusters at Low Temperatures†. The Journal of Physical Chemistry B. 2005;109(6):2155-63.
 19. Topics in Catalysis. 2003;22(1/2):9-15.
 20. Tougerti A, Cristol S, Berrier E, Briois V, La Fontaine C, Villain F, et al. XANES study of rhenium oxide compounds at the L₁ and L₃ absorption edges. Physical Review B. 2012;85(12).
 21. Liu H, Iglesia E. Selective One-Step Synthesis of Dimethoxymethane via Methanol or Dimethyl Ether Oxidation on H₃+nVnMo₁₂-nPO₄ Keggin Structures. The Journal of Physical Chemistry B. 2003;107(39):10840-7.
 22. Jingwei Liu YF, Qing Sun, Jianyi Shen. TiO₂ nanotubes supported V₂O₅ for the selective oxidation of methanol to dimethoxymethane. Microporous and Mesoporous Materials. 2008;116(1-3):614-21.
 23. Golinska-Mazwa H, Decyk P, Ziolk M. Sb, V, Nb containing catalysts in low temperature oxidation of methanol - The effect of preparation method on activity and selectivity. Journal of Catalysis. 2011;284(1):109-23.
 24. Rowsell JLC, Yaghi OM. Metal-organic frameworks: a new class of porous materials. Microporous and Mesoporous Materials. 2004;73(1):3-14.
 25. Ricco R, Malfatti L, Takahashi M, Hill AJ, Falcaro P. Applications of magnetic metal-organic framework composites. Journal of Materials Chemistry A. 2013;1(42):13033.
 26. Maya F, Palomino Cabello C, Estela JM, Cerdà V, Turnes Palomino G. Automatic In-Syringe Dispersive Microsolid Phase Extraction Using Magnetic Metal-Organic Frameworks. Analytical Chemistry. 2015;87(15):7545-9.
 27. Tuan. A. Vu GHL, Canh. D. Dao, Lan. Q. Dang, Kien. T. Nguyen, Phuong. T. Dang, Hoa. T. K. Tran, Quang. T. Duong, Tuyen. V. Nguyen, Gun. D. Lee. Isomorphous substitution of Cr by Fe in MIL-101 framework and its application as a novel heterogeneous photo-Fenton catalyst for reactive dye degradation. RSC Adv. 2014;4(78):41185-94.
 28. Masoomi MY, Beheshti S, Morsali A. Mechanochemical synthesis of new azine-functionalized Zn(II) metal-organic frameworks for improved catalytic performance. J Mater Chem A. 2014;2(40):16863-6.
 29. Corma HGaFXLiX. Engineering Metal Organic Frameworks for Heterogeneous Catalysis. Chemical Reviews. 2010;110(8):4606-55.
 30. Zhang X, Zang XH, Wang JT, Wang C, Wu QH, Wang Z. Porous carbon derived from aluminum-based metal organic framework as a fiber coating for the solid-phase microextraction of polycyclic aromatic hydrocarbons from water and soil. Microchimica Acta. 2015;182(13-14):2353-9.
 31. Liu X, Wang C, Wang Z, Wu Q, Wang Z. Nanoporous carbon derived from a metal organic framework as a new kind of adsorbent for dispersive solid phase extraction of benzoylurea insecticides. Microchimica Acta. 2015;182(11-12):1903-10.
 32. Masoomi MY, Morsali A. Sonochemical synthesis of nanoplates of two Cd(II) based metal-organic frameworks and their applications as precursors for preparation of nano-materials. Ultrasonics Sonochemistry. 2016;28:240-9.
 33. Masoomi MY, Bagheri M, Morsali A. High adsorption capacity of two Zn-based metal-organic frameworks by ultrasound assisted synthesis. Ultrasonics Sonochemistry. 2016;33:54-60.
 34. Masoomi MY, Morsali A. Applications of metal-organic coordination polymers as precursors for preparation of nano-materials. Coordination Chemistry Reviews. 2012;256(23):2921-43.
 35. Raoof F, Taghizadeh M, Eliassi A, Yaripour F. Effects of temperature and feed composition on catalytic dehydration of methanol to dimethyl ether over γ-alumina. Fuel. 2008;87(13):2967-71.
 36. Haque E, Jun JW, Jung SH. Adsorptive removal of methyl orange and methylene blue from aqueous solution with a metal-organic framework material, iron terephthalate (MOF-235). Journal of Hazardous Materials. 2011;185(1):507-11.
 37. Shi J, Hei S, Liu H, Fu Y, Zhang F, Zhong Y, et al. Synthesis of MIL-100(Fe) at Low Temperature and Atmospheric Pressure. Journal of Chemistry. 2013;2013:1-4.
 38. Haul R. S. J. Gregg, K. S. W. Sing: Adsorption, Surface Area and Porosity. 2. Auflage, Academic Press, London 1982. 303 Seiten, Preis: \$ 49.50. Berichte der Bunsengesellschaft für physikalische Chemie. 1982;86(10):957-.
 39. Royer S, Sécordel X, Brandhorst M, Dumeignil F, Cristol S, Dujardin C, et al. Amorphous oxide as a novel efficient catalyst for direct selective oxidation of methanol to dimethoxymethane. Chem Commun. 2008(7):865-7.
 40. Lu X, Qin Z, Dong M, Zhu H, Wang G, Zhao Y, et al. Selective oxidation of methanol to dimethoxymethane over acid-modified V₂O₅/TiO₂ catalysts. Fuel. 2011;90(4):1335-9.